Physiological Measurement

Single-source PPG based local pulse wave velocity measurement: A potential cuffless blood pressure estimation technique

To cite this article before publication: Nabeel P M *et al* 2017 *Physiol. Meas.* in press https://doi.org/10.1088/1361-6579/aa9550

Single-source PPG based local pulse wave velocity measurement: A potential cuffless blood pressure estimation technique

P M Nabeel[1], J Jayaraj[2] and S Mohanasankar[1,2]

[1]Department of Electrical Engineering, Indian Institute of Technology (IIT) Madras, Chennai, India

[2]Healthcare Technology Innovation Centre (HTIC), IIT Madras, Chennai, India

Email: nabeelnpm@gmail.com, ee13d213@ee.iitm.ac.in

Abstract

Objective: A novel photoplethysmograph (PPG) probe employs dual photodiodes excited using single infrared light source was developed for local Pulse Wave Velocity (PWV) measurement. The potential use of proposed system in cuffless Blood Pressure (BP) techniques was demonstrated. *Approach:* Initial validation measurements were performed on a phantom using a reference method. Further, an in-vivo study was carried out in 35 volunteers (age = 28±4.5 years). Carotid local PWV, carotid to finger Pulse Transit Time (PTT_R) and Pulse Arrival Time at the carotid artery (PAT_C) were simultaneously measured. Beat-by-beat variation of local PWV due to BP changes was studied during post-exercise relaxation. Cuffless BP estimation accuracy of local PWV, PAT_C, and PTT_R was investigated based on inter- and intra-subject models with best-case calibration. *Main results:* Accuracy of the proposed system, hardware inter-channel delay (< 0.1 ms), repeatability (beat-to-beat variation = 4.15% - 11.38%) and reproducibility of measurement (r = 0.96) were examined. For the phantom experiment, measured PWV values did not differ by more than 0.74 m/s compared to the reference PWV. Better correlation was observed between brachial BP parameters versus local PWV (r = 0.74 – 0.78) compared to PTT_R (|r| = 0.62 – 0.67) and PAT_C (|r| = 0.52 – 0.68). Cuffless BP estimation using local PWV was better than PTT_R and PAT_C with population-specific models. More accurate estimates of arterial BP levels were achieved using local PWV via subject-specific models (root-mean-square-error ≤ 2.61 mmHg). *Significance:* A reliable system for cuffless BP measurement and local estimation of arterial wall properties.

Keywords: Blood pressure, Cuffless BP, local PWV, photoplethysmograph, PPG, pulse arrival time, pulse transit time, pulse wave velocity

1. Introduction

Arterial Blood Pressure (BP) measurement in routine clinical diagnostic practice and hypertension management is often performed using cuff-type manometers. The conventional cuff-based methods (auscultatory and oscillometric techniques) provide only intermittent pressure levels with systolic and diastolic values. Short- or long-term continuous BP monitoring and BP variability have been well-recognized as an accurate determinant of cardiovascular diseases (Ding *et al* 2016, Peter *et al* 2014). The conventional cuff-based devices cannot be directly used for continuous BP monitoring and tracking of beat-to-beat variations. Continuous measurement of finger arterial pressure has been developed based on the volume-clamp method

using a finger cuff and an inflatable bladder (Bogert *et al* 2005). However, all cuff-based BP assessment techniques are known to suffer from several limitations (Buxi *et al* 2015).

Cuff-less techniques for continuous BP measurement involving arterial pressure and flow wave dynamics are widely pursued (Ding *et al* 2016, Mukkamala *et al* 2015). A number of approaches for continuous cuff-less BP measurement have been developed using regional Pulse Wave Velocity (PWV), Pulse Transit Time (PTT) and Pulse Arrival Time (PAT) (Mukkamala *et al* 2015). However, the accuracy and reliability of cuffless BP techniques using regional transit time estimates are limited due to the following reasons; (a) variation of pre-ejection period in PAT with cardiac electro-mechanical properties (Martin *et al* 2016), (b) Regional PWV and PTT obtained from two distinct arterial sites with different mechanical characteristics provide only an average estimate (Pereira *et al* 2015), (c) Coarse approximation of the pulse propagation distance in regional PWV assessment (Pereira *et al* 2015, Boutouyrie *et al* 2009) constituting error in estimated BP parameters, (d) Biomechanical equations relating flow wave dynamics and BP parameters hold true only when no wave reflections occur (Bramwell and Hill 1922, Westenberg *et al* 2012). These inherent sources of error in regional estimates create the necessity for frequent subject- and/or population-specific recalibration and hence, limit the use of such devices in routine clinical diagnostic practice (Mukkamala *et al* 2015, McCarthy *et al* 2013, Ding *et al* 2016). It is necessary to overcome aforementioned shortcomings to develop an accurate cuff-free system for continuous BP measurement.

Studies have reported that PWV measurement made on a small segment of an artery (local PWV) represent the true blood pulse propagation velocity (Pereira *et al* 2015, Hermeling *et al* 2010). Precisely measured local PWV values are free from error due to a coarse approximation of propagation distance and multiple wave reflections. Hence, it can be considered as a better marker of arterial pressure levels. In this work, we propose a novel photoplethysmograph (PPG) probe for local PWV measurement. The design consists of two photodiodes placed at adjacent measurement points, excited using a single infrared light source (single-source PPG transducer). A prototype device was developed to demonstrate the feasibility of capturing dual PPG signals and beat-by-beat local PWV measurement using single-source PPG probe. Performance and measurement accuracy of the developed local PWV device was initially validated by conducting in-vitro experiments on a phantom. Real-time signal acquisition, repeatability and reproducibility of the device were further validated on 35 human volunteers. The efficiency of the device to detect beat-to-beat variation in local PWV due to arterial pressure changes was verified on young and healthy volunteers during their post-exercise recovery period. Further, cuffless estimation of arterial BP levels using local PWV with inter- and intra-subject mathematical models was demonstrated. It was also the objective of this study to assess carotid to finger PTT (PTT_R) and arrival time of pulse wave at the carotid artery (PAT_C) so that it could be compared with local PWV as markers of arterial BP levels.

2. Design of single-source PPG transducer

The proposed single-source PPG probe design has a specific functional structure: two highly sensitive photodiodes symmetrically placed at precise and well-known distance on either side of a single light source. A narrow beam Infrared Light Emitting Diode (IR LED) was used as the light source to illuminate the arterial site under measurement. Infrared wavelength was preferred to ensure deeper penetration of light into the tissue owing to its lower absorption by pigmentation (Cai *et al* 2008, Delpy *et al* 1997). Photodiodes were able to capture reflected light from two distinct measurement locations. The output signals represent underlying blood pulse wave propagation through the illuminated artery (reflectance photoplethysmography principle). A significant transit time delay was observed between simultaneously acquired dual pulse waveforms. This blood pulse transit time delay obtained from a smaller arterial section was used for local PWV measurement. The initial prototype design was optimized for local PWV measurement from the carotid site (carotid local PWV). The carotid artery was preferred since it

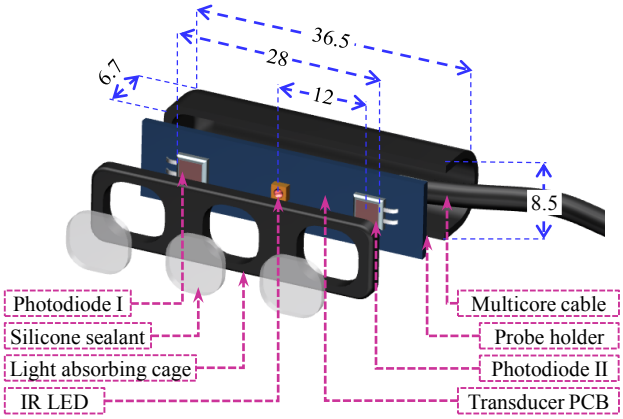

Figure 1. Single-source PPG transducer assembly (all dimensions are in mm).

closely represents the central aortic conditions, is easily accessible and offers a straight branch-free pathway before the bifurcation.

A three-dimensional (3D) sketch of sensor assembly and packaging of the single-source PPG transducer has been presented in figure 1. The IR LED (OSRAM Opto Semiconductors – SFH 4451, 850 nm) was soldered at the middle of a custom designed rectangular (36 mm × 8 mm) transducer printed circuit board (PCB). Two highly sensitive photodiodes with 16 mm^2 window size (OSI Optoelectronics – 16 CSL) were also soldered on the transducer PCB. Multiple trials on different subjects were conducted to finalize the center-to-center separation distance (δ) between IR LED and photodiodes. Initial experiment results revealed that the sensor arrangement with δ less than 6 mm does not provide adequate penetration depth for incident light. As a result, PPG probe was not able to detect arterial pulsations. Simultaneous acquisition of dual pulse signal from multiple subjects was difficult when δ greater than 20 mm. Hence, an optimum distance of δ = 12 mm was used in the present prototype design.

The IR LED was driven by a high current (more than 45 mA) such that the light intensity was sufficient to obtain dual PPG signals irrespective of artery depth and thickness of tissue layer above the artery. IR LED and photodiodes were kept inside a black colored light absorbing cage. It was used to avoid the permanent saturation of photodiodes due to the direct coupling of incident infrared light. Optimized cage dimensions with 5 mm thick isolating barrier between the IR LED-photodiode pair was preferred. Transducer PCB and isolation cage were attached and enclosed in probe holder. Finally, IR LED and photodiodes were coated with a transparent general purpose silicone sealant (Wacker-GP). Silicone coating on light source and detectors help to maintain optical continuity between sensing area and the skin surface. The overall size of the developed single-source PPG probe was 36.5 mm × 8.5 mm × 6.7 mm with 28 mm end-to-end distance between the active windows of photodiodes.

3. Signal acquisition and processing

3.1. Analog front-end hardware features

Arterial blood pulse signal acquired using PPG transducers consists of both static (DC) and pulsating (AC) components (Kamal *et al* 1989, Lindberg and Öberg 1993). The DC component of PPG signal is proportional to total blood volume in the measurement area. AC component is synchronized with the cardiac cycle and follows arterial blood volume and flow changes. AC component of PPG signal is typically less than 0.2% of DC amplitude. Removal of DC from the PPG waveforms was mandatory for the amplification of AC components without causing permanent saturation of amplifiers. In practice, it not straightforward to remove DC components from the PPG signals without introducing any additional signal propagation delay. Direct use of resistor-capacitor based signal conditioning filters for DC elimination causes significant inter-channel delay due to the mismatch between their characteristic time constants. A non-zero inter-

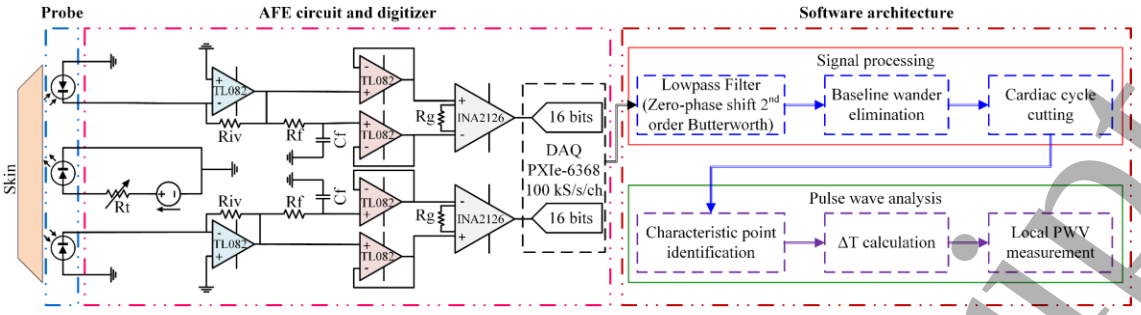

Figure 2. Local PWV measurement system block diagram indicating the internal circuit of single-source PPG probe, AFE and software architecture.

channel delay was critical for transit time delay measurements employing sensors placed in close proximity. Hence, an analog front-end (AFE) circuit with negligible inter-channel delay and a high-speed signal acquisition module were desired for reliable blood pulse detection.

An application-specific dual-channel AFE was designed and developed for simultaneous acquisition of PPG signals. The basic circuit schematic of the AFE, internal circuit diagram of single-source PPG probe and software architecture of proposed measurement system has been described in figure 2. The proposed AFE design was primarily focused on reducing the inter-channel delay between analog channels. Extraction of pulsatile components from the raw blood pulse signals using DC subtraction (without any signal conditioning filters and energy storage elements in the principal signal path) significantly reduces the inter-channel delay (Nabeel *et al* 2017). As illustrated in figure 2, the output current signals from photodiodes of PPG transducers were initially converted into a voltage signal using transimpedance amplifiers. Average DC voltage of PPG signal was extracted using an R-C network (corner frequency = 0.05 Hz) implemented in the parallel signal path. Raw PPG signal and its average DC voltage level from each channel were given to the V_{IN}^{+} and V_{IN}^{-} input terminals of precision instrumentation amplifiers (Texas Instruments – INA2126) respectively, via Opamp (Texas Instruments – TL082CP) based voltage buffers. Subtraction of the DC component from original PPG signal and further amplification (gain ≈ 40 dB) was performed by the instrumentation amplifier. Amplified PPG signals were digitized using a simultaneous sampling data acquisition (DAQ) module (National Instruments® – PXIe-6368). Signals were continuously acquired at a sampling rate of 100 kS/s/ch with 16-bit resolution. Use of a simultaneous sampling DAQ card with high sampling rate helped to eliminate any mismatch due to digital pipelining, data transfer delays and timing error arising from the system sampling clock.

3.2. Software architecture and signal processing

Signal acquisition and processing were performed by a custom program developed using LabVIEW (National Instruments®). Digital domain processing, transit time measurement, and PWV calculation were automatically performed. The measurement algorithm (figure 2) was divided into two steps: signal processing and pulse wave analysis. In the signal processing stage, acquired PPG waveforms were low-pass filtered using Butterworth 2nd order digital filter. Since the expected range of blood pulse signal frequency in human is from 0.7 Hz to 3 Hz, the low-pass filter was realized with 10 Hz cut-off frequency, thus allowing the fundamental and at least two harmonics, while eliminating the out-of-band noise. Zero phase difference between raw signal and the filtered signal was ensured by applying filter operation in the forward and backward direction (zero-phase shift filter operation). Further, the baseline drift of the PPG waveforms caused by body movement and respiration was removed using wandering removal process (Fedotov *et al* 2014). Finally, cycle cutting was performed to separate each beat from the signal train and to collate the corresponding proximal and distal cardiac cycle pairs. For this, the diastolic minimum points of proximal PPG signal were automatically detected from each beat. 50 ms prior to the diastolic minimum was taken as the fiducial point for cycle cutting.

Time axis of the proximal and distal cardiac cycle pairs was synchronized by taking same fiducial points in both channels. These cycle pairs were used for beat-by-beat local PWV measurement. The LabVIEW program also provides provision for real-time signal storage of acquired waveforms for future reference.

3.3. Pulse wave analysis

The arterial pulse signal is composed of a forward moving blood pulse wave superimposed with reflected signals from various bifurcation points in the arterial tree (Boutouyrie *et al* 2009). The reflected signals voyage with different propagation velocity and amplitude. Depending on the arterial sites, the reflected signals alter the shape and timing information of original pulse signal. Since the early systolic region of blood pulse is minimally affected by the reflected waves (Hermeling *et al* 2007), the characteristic points for transit time measurements are often selected from this region. Characteristic points are specific identification points based on the physiological features of blood pulse waveform. The time delay between characteristic points of proximal and distal cycle pair is referred to as transit time (ΔT). Therefore, precise identification of characteristic points is highly desirable for accurate ΔT and PWV calculation.

3.3.1. Characteristics point identification. The second derivative maximum technique (Kazanavicius *et al* 2015) was implemented for characteristic point identification. It was reported as an efficient method for repeatable measurements (Chiu *et al* 1991). The second derivative maximum technique uses the point at which the second derivative of a blood pulse cycle is maximal as its characteristic point. It is typically close to the systolic foot position, where the change in slope is maximum. For a given cardiac cycle with dataset values (Ψ) collected at time intervals (t) having a finite sample number (k), the second derivative can be determined using the formula,

$$\frac{d^2\Psi}{dt^2} = \frac{(\Psi_{k+1}-\Psi_k)-(\Psi_k-\Psi_{k-1})}{\frac{1}{2}(t_{k+1}-t_{k-1})} \quad (1)$$

3.3.2. Local ΔT and PWV measurement. The pulse wave analysis phase emphasized on accurate measurement of ΔT to obtain reliable carotid local PWV values. Using characteristic point detection algorithm, local ΔT was calculated from the fiducial points of proximal and distal carotid pulse cycle pair (figure 3). Centre-to-centre distance between the photodiodes was taken as blood pulse propagation distance (ΔD). Within a small distance (ΔD = 24 mm), the carotid artery was assumed to be a homogeneous section with no curvature. Finally, carotid local PWV was estimated from each cardiac cycles in a beat-by-beat manner using (2).

$$\text{Local PWV} = \frac{\Delta D}{\Delta T} \quad (2)$$

3.4. Finger PPG and ECG signal acquisition

Real-time finger PPG and ECG signals were also acquired along with dual carotid PPG for simultaneous measurement of local PWV, PTT_R, and PAT_C. Synchronized acquisition of all four waveforms was performed by the developed local PWV measurement system advanced with two sub-units: one for the finger PPG signal acquisition and another one for real-time ECG signal acquisition. Carotid PPG AFE design was replicated in finger PPG channel for signal acquisition using transmittance type fingertip PPG probe. Reference ECG signal was acquired using a commercial three electrodes system with fully integrated single-lead AFE (Analog Devices Inc. – AD8232). Signals were digitized using a simultaneous sampling DAQ card (National Instruments® – PXIe-6368) at a sampling rate of 100 kS/s/ch. The signal processing software was also modified for simultaneous measurement of local PWV, PTT_R, and PAT_C. As illustrated in figure 3, PTT_R was determined as the time delay between fiducial points of proximal carotid PPG signal and finger PPG signal. PAT_C was determined as the time delay

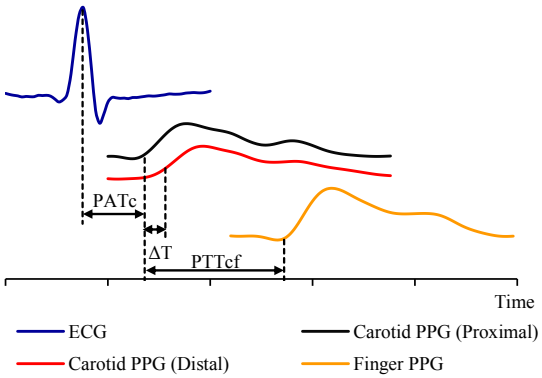

Figure 3. Determination of various blood pulse transit time estimates from simultaneously acquired biopotential signals.

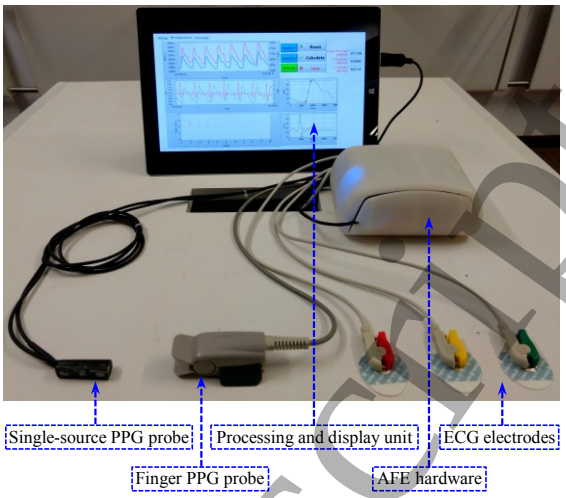

Figure 4. Single-source PPG probe and local PWV device with ECG and finger PPG modules. A screenshot of GUI is shown in the display unit.

between R peak of QRS complex of ECG and fiducial point of the proximal carotid PPG waveform. Figure 4 shows the developed prototype of single-source PPG based local PWV device advanced with ECG and finger PPG signal acquisition modules.

4. In-vitro validation technique and results

Design efficiency and functionality of the single-source PPG probe and proposed local PWV device were experimentally validated by an in-vitro study. The study was performed using a commercially available manikin phantom with realistic carotid artery anatomy (Blue Phantom-CAE Healthcare – BPIJ500-C). Figure 5(a) presents the experimental setup of the performed in-vitro validation study. Arterial pulsations were manually simulated by controlled and repetitive pumping of the provided hand bulb. The study comprised the recording of phantom pulse waveforms, and assessment of pulse propagation velocity of blood mimicking fluid through the phantom (PWV_P) using single-source PPG transducer (measured PWV_P) and a reference method (reference PWV_P). Conventional two-point PWV measurement technique using dual pressure waves from identical tonometers (Millar® Instruments – SPT-301) was considered as the reference method (Salvi *et al* 2008, Nabeel *et al* 2017). Both the tonometers (uncalibrated) were rigidly fixed on the neck above the carotid artery of the phantom model with a separation of 70 mm. The single-source PPG probe was adhered to the phantom between the tonometers using a transparent two-sided adhesive tape as shown in figure 5(a).

Phantom pulse waveforms detected by the single-source PPG transducer was acquired and processed using the prototype local PWV device. Tonometer signal acquisition and processing were performed using ADInstruments' LabChart software via Bridge Amp and PowerLab. Simultaneously acquired proximal and distal phantom pulse waveforms from the tonometers and single-source PPG probe are shown in figure 5(b) and figure 5(c) respectively, exhibiting same average pulse rate. Figure 5(d) depicts the reference and measured PWV_P values along with their difference (reference PWV_P – measured PWV_P), obtained from continuous phantom pulse cycles simulated at various pressure level. 80% of the measurements were within an error band of ±0.5 m/s, and the maximum difference between the reference and measured PWV_P was 0.74 m/s. Both methods correlated significantly ($r = 0.97$, $p < 0.001$). The Bland-Altman analysis (figure 5(e)) revealed a non-significant bias of –0.015 m/s with standard deviation (SD) of differences equal to ±0.38 m/s. Validation measurements in the phantom demonstrated the expected functionality of single-source PPG probe and associated measurement system. The proposed device found to allow accurate and reliable estimation of local PWV in a non-invasive and continuous manner.

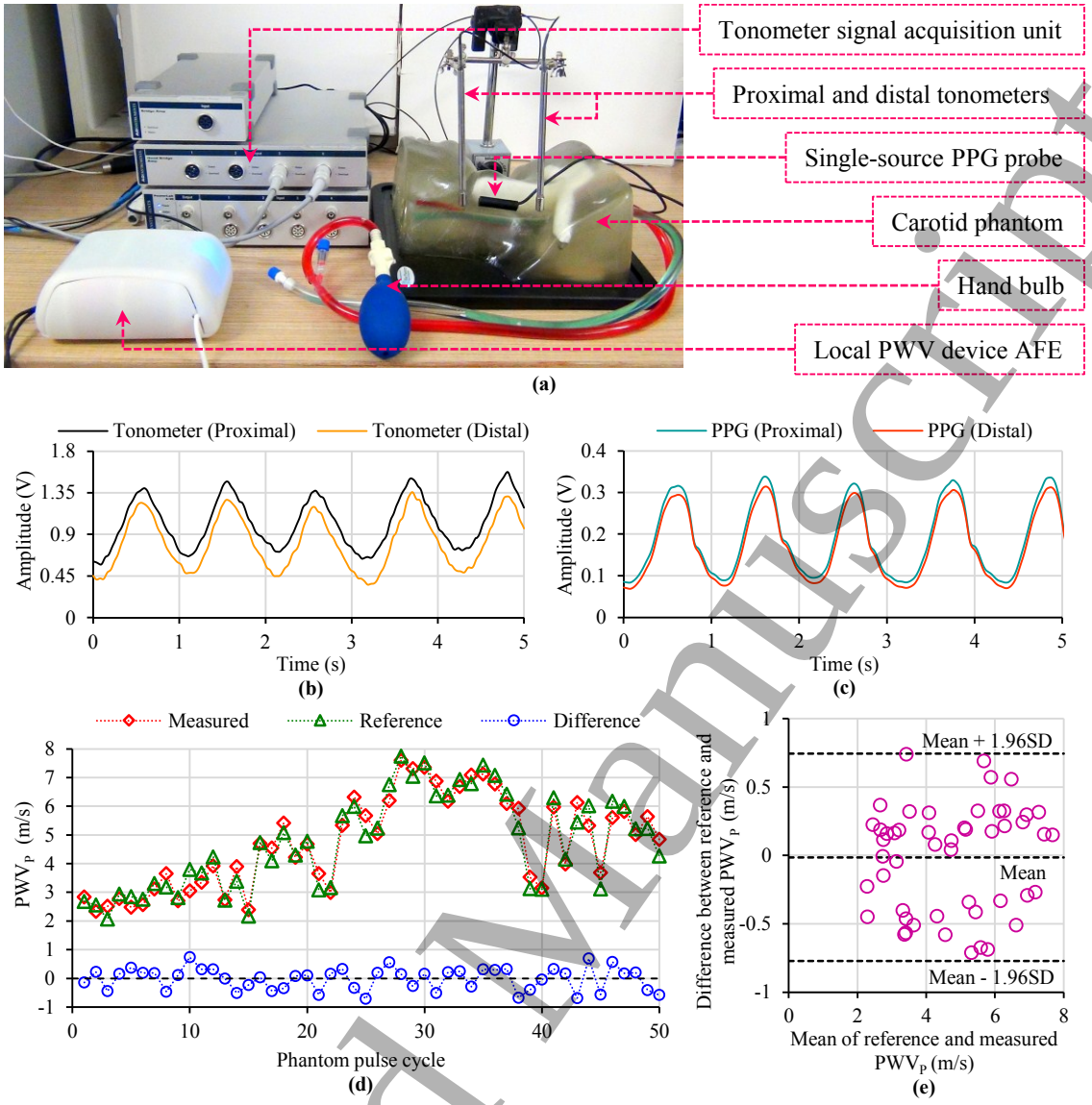

Figure 5. (a) In-vitro validation experimental setup. (b) A sample of phantom pulse waveforms collected by the proximal and distal tonometers. (c) A sample of phantom pulse waveforms collected by the single-source PPG probe. (d) Cycle-by-cycle PWV_P recorded using reference method and device under test at various pressure level. (e) Bland-Altman plot of the comparison between reference and measured PWV_P.

5. In-vivo validation materials and methods

5.1. Study objectives

- To verify the efficiency of the single-source PPG probe and associated measurement system for continuous signal acquisition, repeatable and reproducible local PWV measurement from multiple subjects.
- To perform an inter-subject correlation analysis of carotid local PWV, PTT_R, and PAT_C versus brachial BP parameters.
- To examine the proposed local PWV device regarding its ability to measure the beat-by-beat variation of local PWV due to BP changes in individual subjects.
- To test the cuffless BP estimation accuracy of the proposed system with inter- and intra-subject models after best-case calibration.

5.2. Subject selection

Thirty-five normotensive subjects (age = 28±4.5 years; gender: 23 males and 12 females; height = 168±12 cm; weight = 73±15 kg) were recruited for the in-vivo validation study. Written informed consent was obtained from all participants after explaining the study objective and protocol. Anthropometric measurements were initially taken and recorded in the subject database. Participants were requested to take 5 min rest in a temperature controlled room (23±2°C) before the study to achieve a steady heartrate and BP state.

5.3. In-vivo study protocol

5.3.1. Blood pulse signal acquisition and local PWV measurement. Local PWV measurement was performed on left common carotid artery (sitting posture) by a single operator. Single-source PPG probe was placed at the carotid site after identifying the artery by palpation. Probe placement and orientation were adjusted to acquire dual PPG waveforms. Beat-by-beat local PWV value was recorded for 30 seconds on each subject for repeatability test.

5.3.2. Local PWV reproducibility evaluation. Reproducibility of the proposed system was tested by performing sequential measurement of local PWV. Consecutive measurements were taken from each volunteer by the same operator for a fixed time interval (15 seconds) with a small break (10 seconds) between each trial. Mean local PWV values of consecutive trials were used for intra-operator reproducibility analysis.

5.3.3. BP measurement from the brachial artery. Brachial BP measurement on the left arm using a pressure cuff was performed at various stages throughout the validation study. A clinical grade automated oscillometric BP apparatus (SunTech® 247™) was used for Systolic Blood Pressure (SBP), Diastolic Blood Pressure (DBP) and Mean Arterial Pressure (MAP) measurement. Average BP values of two consecutive trials were used for analysis.

5.3.4. Simultaneous measurement of local PWV, PTT_R, and PAT_C. Once the data collection for repeatability and reproducibility analysis was finished, volunteers were prepared with sensors for local PWV, PTT_R, and PAT_C measurement. As explained in the previous section, carotid PPG signals were recorded using single-source PPG probe. A commercially available SpO_2 clip (NellcorTM – DS100A) was attached to the left index finger for finger PPG. Disposable ECG skin electrodes with pre-gelled Ag/AgCl sensors were placed on the left hand, right hand and right leg for ECG signal. Brachial BP was recorded before the signal acquisition. Beat-by-beat carotid local PWV, PTT_R and PAT_C were simultaneously measured for 30 seconds. Respective mean values and brachial BP obtained from all 35 subjects were used for correlation analysis and to develop inter-subject cuffless BP models.

5.3.5. Local PWV measurement during post-exercise relaxation. An exercise study was conducted to verify the ability of proposed device to detect local PWV variations due to arterial pressure changes. Only those individuals with age less than 30 years and no history of any serious diseases were recruited for this study (7 subjects; age = 24±3 years). After the baseline measurements, volunteers were subjected to running exercise on a treadmill (Afton – XO-150). Starting from minimum speed (1 km/h), exercise continued for 10 min at various speed levels (maximum up to 10 km/h). Volunteers were comfortably seated after the exercise for complete relaxation. During this period, local PWV was continuously acquired from the left carotid artery, and brachial BP was measured at regular time intervals. Measurements were recorded until BP returned to the baseline value or remained steady. The data collected from the exercise study was used to develop intra-subject models for cuffless BP measurement. These models were tested using the second dataset of baseline BP and local PWV values collected at random time intervals from same subjects during their routine work.

6. In-vivo study results and discussion

6.1. Measurement accuracy and potential error sources

Before the detailed analysis of in-vivo study observations and results, a brief discussion about the accuracy of the measurement system and potential error sources in the recorded carotid local PWV are presented. Ambiguity in ΔD was controlled by precision placement of photodiodes during the final transducer assembly process. ΔD (= 24 mm) was measured using a digital Vernier caliper (Mitutoyo – Digimatic Caliper - CD-6"VC) with an instrumental error of ±0.03 mm. Hence, a maximum of 0.125% error in ΔD ($\%\varepsilon_{\Delta D}$ = 0.125%) was expected in the prototype design of single-source PPG probe.

Hardware inter-channel delay and system sampling clock can introduce timing errors in local PWV estimates. Inter-channel delay obtained from five selected subjects with different heartrate and BP is presented in figure 6. It was measured by feeding carotid PPG signal from a single sensor to both the input channels simultaneously. The band inside each box in figure 6 indicate the median of inter-channel delay values obtained from multiple cycles. Bottom and top of the boxes indicate the first and third quartiles with vertical lines extending to the minimum and the maximum delay values respectively. A maximum of 1.8% error in local ΔT ($\%\varepsilon_{\Delta T}$ = 1.8%) was expected due to hardware inter-channel delay. Timing errors caused by the sampling of acquisition module (sampling rate = 100 kS/s/ch; clock period = 10 μs) was insignificant when compared to the expected local ΔT values. Further, the tissue transit time of infrared light wave is much shorter than the blood pulse transit time. Any difference in tissue transit time at two measurement locations can be neglected due to similar skin and tissue composition within a small section. Therefore, the expected error in carotid local PWV ($\%\varepsilon_{\text{local PWV}} = \%\varepsilon_{\Delta D} + \%\varepsilon_{\Delta T}$) due to hardware limitations was less than 2%.

6.2. Reliability of carotid blood pulse signal acquisition

Proximal and distal blood pulse signals for local PWV measurement was acquired from multiple subjects under different physiological conditions. Measurement algorithm was susceptible to the quality of the acquired blood pulse waveforms. The prototype device was able to acquire dual PPG waveforms with signal-to-noise ratio approximately 28 dB, which was adequate for reliable local ΔT measurement using the second derivative maximum technique (Solà *et al* 2009). Figure 7 exhibits carotid blood pulse waveforms (after signal conditioning) acquired from a volunteer (age = 26 years, body mass index (BMI) = 25.05 kg/m^2, SBP/DBP = 118/73 mmHg). Competency of the single-source PPG transducer to acquire distinct pulse waveforms from adjacent sites makes the proposed design perfect for local PWV measurement. The peak-to-peak amplitude of raw pulse waveforms was subjective and varied between 6 to 17 mV_{PP} in individual subjects during the present study. Inter-beat period of acquired PPG signals was

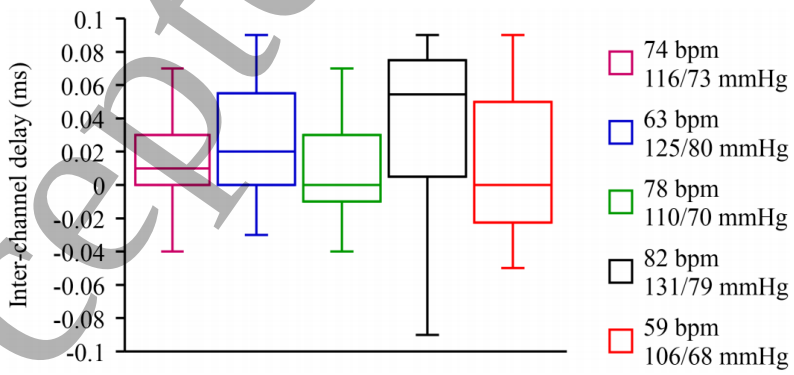

Figure 6. Box-and-whisker plot of beat-by-beat hardware inter-channel delay obtained from five subjects. Respective heartrate (in bpm) and SBP/DBP (in mmHg) of each subject are shown in the figure.

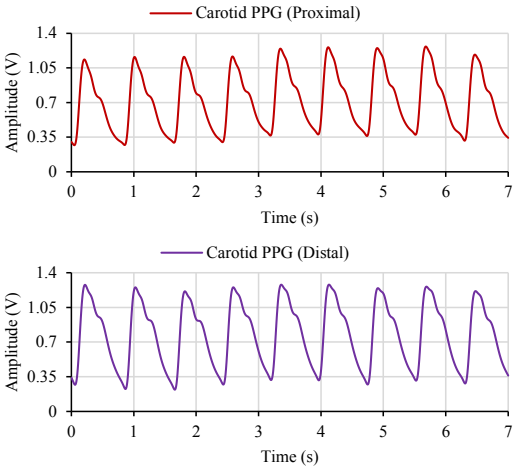

Figure 7. Simultaneously acquired proximal and distal carotid PPG waveforms of a particular volunteer using single-source PPG transducer.

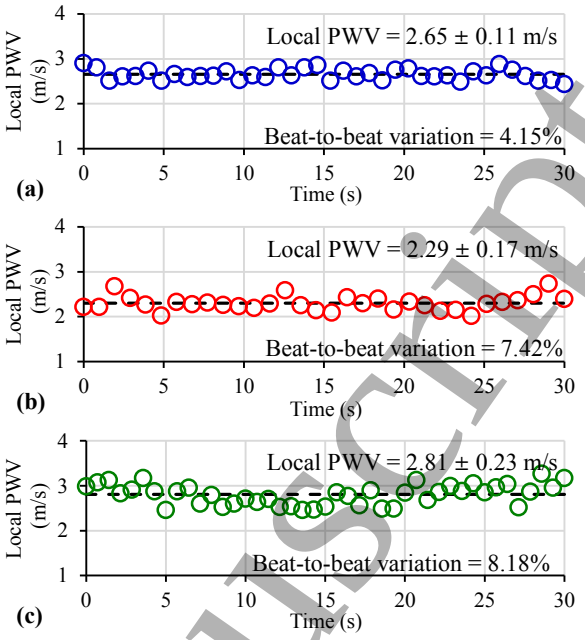

Figure 8. Beat-to-beat variation of carotid local PWV of three different subjects. (a) Age = 26 years, BMI = 25.05 kg/m^2. (b) Age = 24 years, BMI = 26.76 kg/m^2. (c) Age = 24 years, BMI = 30.96 kg/m^2.

compared against R-R interval of ECG waveform to ensure reliability. Mean absolute error in inter-beat period measurement was less than 0.14%.

6.3. Repeatability and reproducibility of carotid local PWV measurement

The prototype design of single-source PPG probe was efficient and facilitates easy measurement of beat-by-beat carotid local PWV. Artery detection, probe placement and orientation procedures, signal acquisition, and measurement process were completed within 2 min. Baseline carotid PWV estimates were less compared to previously reported carotid-to-femoral and carotid-to-radial PWV (Reusz *et al* 2010). Mean carotid local PWV values obtained from 35 subjects were in the range of 2.52±0.41 m/s. It was consistently observed for multiple subjects with high reproducibility under various physiological conditions. The obtained values were comparable with carotid PWV reported in previous studies using ultrasound and accelerometer transducers (Sorensen *et al* 2008, Faita *et al* 2010). Figure 8(a) to 8(c) shows the recorded beat-by-beat carotid local PWV values of three different volunteers (30 seconds data). Beat-to-beat variation was calculated by dividing their SD with mean and expressing it in percentage. The minimum and maximum beat-to-beat variation observed during the study were 4.15% and 11.38%. Relatively high beat-to-beat variation (7.01% – 11.38%) was observed in subjects with obesity and weak carotid surface pulsations.

Repeated sequential measurement of local PWV by the same operator allowed evaluation of reproducibility of the measurement system. Agreement between two consecutive sets of measurement (Trial I and Trial II) was evaluated via Pearson's correlation coefficient (r) and Bland-Altman analysis. Statistical significance on all tests was indicated by p-value < 0.05. Mean carotid PWV from first set measurement did not differ significantly from the second set for each subject. As illustrated in figure 9(a), the Bland-Altman analysis shows a non-significant bias of 0.02 m/s with an SD of the differences equal to 0.11 m/s. Agreement between the two consecutive measurements from multiple subjects has been depicted in figure 9(b). The correlation between two sets of measurements were highly significant ($r = 0.96$, $p < 0.001$). Study results favor the reproducibility of developed local PWV measurement system.

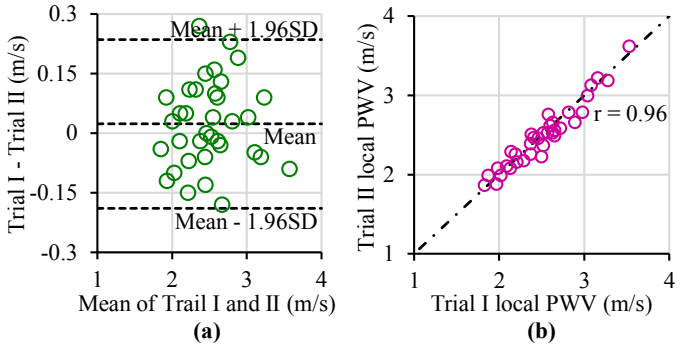

Figure 9. Local PWV reproducibility test results. (a) Bland-Altman plot showing difference between two trials as a function of their average. (b) Correlation plot of Trial I and Trial II.

6.4. Cuffless BP estimation accuracy of local PWV, PTT_R, and PAT_C

Single-source PPG device advanced with finger PPG and ECG sub-units was capable of simultaneous acquisition of required biopotential signals. Reliable estimates of local PWV, PTT_R (beat-to-beat variation < 6.39%) and PAT_C (beat-to-beat variation < 8.01%) were obtained. The absolute value of measured PTT_R and PAT_C were in the range of 229.16±27.96 ms and 86.78±12.61 ms respectively. Mean carotid local PWV, PTT_R, and PAT_C of all recruited volunteers were consolidated along with their brachial BP for statistical analysis and to develop inter-subject mathematical models for cuffless BP measurement. Figure 10(a) to 10(i) shows the relationship between brachial BP parameters (SBP, DBP, and MAP) versus mean local PWV, PTT_R, and PAT_C pooled overall 35 subjects. PTT_R and PAT_C were preferred over respective regional PWV values in cuffless BP models in order to avoid error due to the coarse approximation of distance between the test points (Pereira *et al* 2015).

The logarithmic function provided the best monotonic fit with maximum correlation for the data points of each BP parameter versus each pulse transit time estimates. Inter-subject mathematical models of the form $BP = \phi \ln(\upsilon) + \omega$ (υ can be local PWV or PTT_R or PAT_C; ϕ, ω are population-specific constants), and the absolute value of correlation coefficients (|r|) are summarized in table 1. The correlation coefficients were statistically significant ($p < 0.001$) and all three transit time estimates were able to track BP parameters. However, carotid local PWV showed better correlation ($r > 0.74$) with brachial BP levels than PTT_R (|r| = 0.62 – 0.67) and PAT_C (|r| = 0.52 – 0.68). Inter-subject models derived from the first group of 35 subjects were used for cuffless BP estimation in a different group of 28 subjects (age = 29.5±6 years, gender: 20 males and 8 females; height = 170±9 cm; weight = 75±12 kg). Local PWV, PTT_R, PAT_C and reference brachial BP were recorded from the second group by following the same protocol discussed in Section 5.3.

Cuffless BP estimation accuracy of each transit time estimates was compared with the reference brachial BP via Bland-Altman analysis as well as by computing the root-mean-square-error (RMSE). Comparison study results are presented in table 1. Bland-Altman analysis showed non-significant bias (absolute value < 1.6 mmHg) for all estimated BP values. Carotid local PWV yielded good DBP estimates with a RMSE of 6.33 mmHg; it was 34% and 48% lower than the RMSE observed in cuffless DBP prediction using PTT_R, and PAT_C respectively. Local PWV also provided 23% and 14% lower RMSE for cuffless SBP prediction than PTT_R, and PAT_C respectively. Statistical comparison of reference versus estimated BP parameters was made using Pearson's correlation analysis and Student's paired t-test. The difference between reference and cuffless estimated BP in all nine cases were statistically insignificant ($p > 0.05$). However, local PWV based BP prediction method showed better correlation with reference values (SBP: $r = 0.73$, DBP: $r = 0.79$, MAP: $r = 0.77$; $p < 0.001$). Similar to PTT_R, PAT_C based BP prediction method was moderately correlated with reference BP parameters ($r = 0.59 – 0.66$; $p < 0.05$). For completeness, conventional PAT (pulse arrival time at the fingertip (PAT_R))

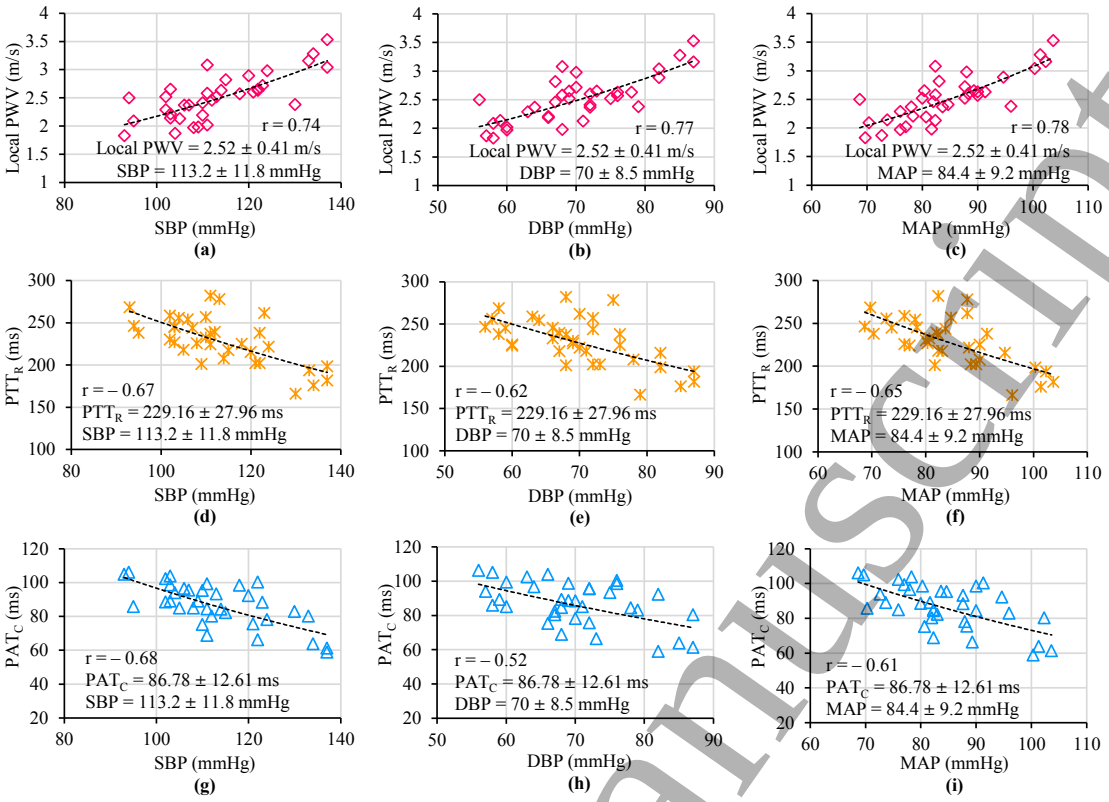

Figure 10. Plots showing the correlation between measured carotid local PWV, PTT_R, PAT_C and brachial SBP, DBP, MAP pooled over all the subjects.

Table 1. Snapshot of pulse transit time estimates versus reference brachial BP |r| values, inter-subject mathematical model and cuffless BP estimation accuracy.

Pulse transit time estimates	BP parameters	|r| - value	Inter-subject cuffless BP estimation model	Comparison of cuffless estimated BP versus reference brachial BP		
				RMSE (mmHg)	Bland-Altman analysis	
					Error bias (mmHg)	SD of error (mmHg)
Local PWV	SBP	0.74	SBP = 53.87 ln(PWV) + 64.12	7.93	1.15	7.98
	DBP	0.77	DBP = 40.39 ln(PWV) + 33.24	6.33	0.86	6.36
	MAP	0.78	MAP = 44.86 ln(PWV) + 43.55	6.74	0.96	6.77
PTT_R	SBP	0.67	SBP = – 64.25 ln(PTT_R) + 461.89	10.34	–1.58	10.41
	DBP	0.62	DBP = –43.15 ln(PTT_R) + 304.17	9.66	–1.07	9.72
	MAP	0.65	MAP = –50.18 ln(PTT_R) + 348.34	9.82	–1.21	9.88
PAT_C	SBP	0.68	SBP = –52.81 ln(PAT_C) + 348.34	9.21	–0.88	9.29
	DBP	0.52	DBP = –29.34 ln(PAT_C) + 200.65	12.11	–1.59	12.25
	MAP	0.61	MAP = –37.17 ln(PAT_C) + 249.88	10.11	–1.14	10.19

acquired from the second group of volunteers was also used to predict the BP parameters. It was mapped through the PAT_R based BP prediction models derived from the first group data. Even with the best possible calibration, PAT_R yielded RMSE > 15 mmHg and $r < 0.55$ ($p < 0.05$) with the reference while estimating cuffless SBP, DBP, and MAP.

6.5. Intra-subject local PWV–BP relationship for cuffless BP measurement

The treadmill-running exercise induced a wide range BP and local PWV variation in individual subjects. Approximately 2.5 – 3.75 times increment in carotid local PWV from the baseline

value and proportional increment in BP parameters were observed after performing the exercise. Instantaneous variation in local PWV due to arterial pressure changes during post-exercise recovery was efficiently tracked by the single-source PPG transducer. Figure 11 displays the post-exercise recovery curve (local PWV, brachial BP parameters, and heartrate as a function of time during the whole recovery period) of one subject (age = 26 years, BMI = 25.05 kg/m^2). Dynamics of the curve such as increment from the baseline value, recovery period and final steady values were depended on individual's physiological factors. Based on the recovery characteristics, post-exercise recovery curve was divided into two phases: (a) transient phase and (b) recovery phase. During the transient phase, local PWV, BP parameters and heartrate decrease rapidly. Local PWV was scattered more in this phase due to heartrate variability, unstable and fast breathing pattern. Local PWV and BP parameters continued to decrease at a lower rate in the recovery phase. Heartrate variability and breathing pattern were fairly stable in the second phase.

Correlation between the intra-subject variation of local PWV versus brachial BP parameters was obtained for each subject. Local PWV correlated equally well with SBP ($r = 0.916 \pm 0.042$, $p < 0.001$), DBP ($r = 0.947 \pm 0.033$, $p < 0.001$) and MAP ($r = 0.929 \pm 0.025$, $p < 0.001$). This statistically significant tight correlation suggested developing cuffless BP technique with intra-subject mathematical models for accurate measurement. Consistent with theory (Mukkamala *et al* 2015, Poon *et al* 2008), a logarithmic function provided the best monotonic fit for pairs of local PWV–BP data points. The developed intra-subject mathematical model was specifically of the form $BP = \Phi \ln(\text{local PWV}) + \Omega$; Φ, Ω are subject-specific constants. Local PWV–BP relationship derived from the post-exercise recovery curve shown in figure 11 has been depicted in figure 12(a) to 12(c). Similar models were developed for each subject by finding the curve that best fitted the data points obtained from their post-exercise recovery curve.

Local PWV values collected from the recruited subjects during their routine work (second dataset) were mapped through their respective mathematical models to predict the BP level. Figure 13(a) to 13(c) illustrates Bland-Altman plots of the error between the cuffless estimated and measured BP levels over all of the subjects (different symbols in the plots correspond to

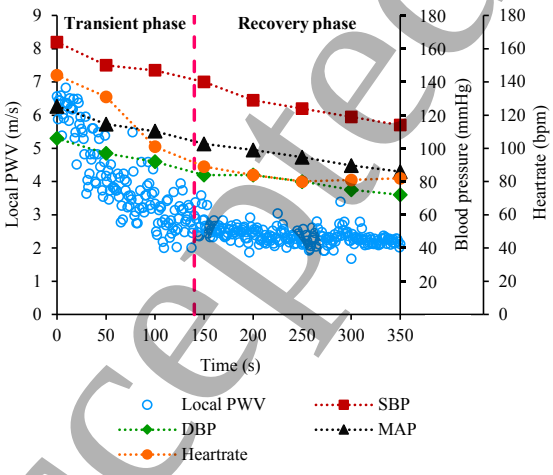

Figure 11. Carotid local PWV, brachial SBP, DBP, MAP and heartrate recorded during the post-exercise recovery period of a subject. Time = 0 s is immediately after treadmill-running exercise.

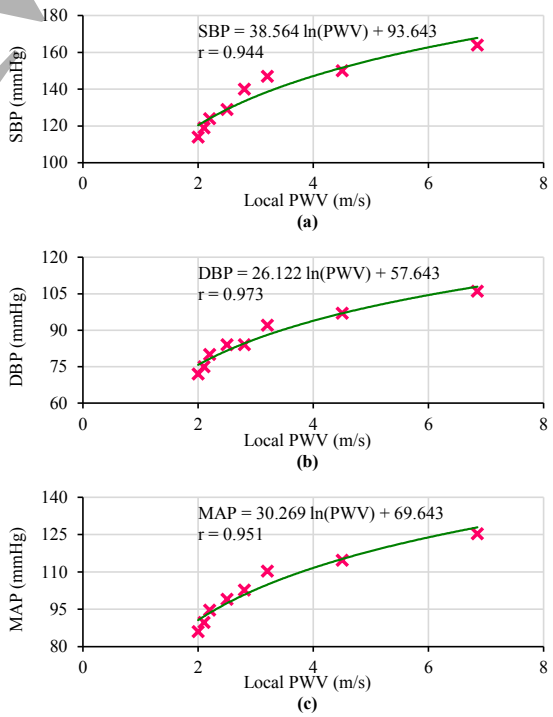

Figure 12. Intra-subject model fitting of (a) SBP versus local PWV, (b) DBP versus local PWV, (c) MAP versus local PWV.

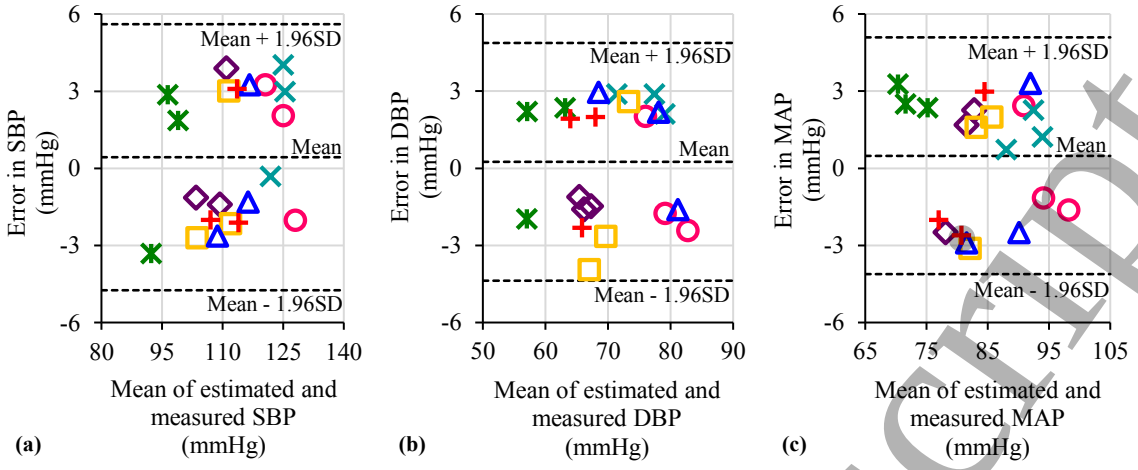

Figure 13. Bland-Altman plots of the error between estimated BP using inter-subject prediction models: (a) SBP, (b) DBP and (c) MAP versus reference brachial BP.

each of the subjects). The proposed technique was able to predict SBP, DBP, and MAP with RMSEs of 2.61 mmHg, 2.32 mmHg, and 2.34 mmHg respectively. The corresponding RMSEs offered by mapping local PWV through inter-subject models were 7.93 mmHg, 6.33 mmHg and 6.74 mmHg (refer table 1). In sum, cuffless techniques based on local PWV using inter-subject models and best-case subject-specific calibration could potentially track arterial BP parameters with a level of acceptable accuracy. By introducing more convenient methods for intra-subject model development and improving form factor (example: single-source PPG patch), the proposed single-source PPG device could be used for cuffless, ambulatory BP monitoring at clinic/home and hypertension screening test.

6.6. Limitations and future efforts

The present in-vivo validation study was conducted on a small population of young and healthy subjects. On the other hand, the current subjects do represent an important sub-population in the sense of early detection of cardiovascular diseases. An extensive validation study with a larger population, recruited from different age group and various pathophysiological sub-populations would confirm and extend these results. Another limitation concerns the applicability of the proposed device for self-monitoring without the assistance of a trained operator. Future efforts are required to implement fully automated intelligent algorithms in the measurement software, to guide the patient regarding probe placement and orientation to acquire dual PPG with the desired signal quality for reliable measurements. Hence, the proposed device would turn out to be a portable, self-monitoring cuffless BP equipment.

7. Conclusion

A prototype single-source PPG probe (dimension = 36.5 mm × 8.5 mm × 6.7 mm) for carotid local PWV measurement was developed and demonstrated. The measurement system consists of an application-specific AFE circuit (inter-channel delay < 0.1 ms), simultaneous sampling data acquisition module (100 kS/s/ch) and fully automated measurement software (developed using LabVIEW). Real-time measurement accuracy of the introduced local PWV device was demonstrated on an arterial flow phantom using dual tonometer reference setup. There was no significant difference between the reference PWV_P and measured PWV_P values (absolute difference ≤ 0.74 m/s, r = 0.97, p < 0.001) The device was further validated by conducting an experimental in-vivo study on 35 subjects. It was able to capture high-fidelity blood pulse signals (signal-to-noise ratio ≈ 28 dB) from small sections of the carotid artery. Carotid local PWV was measured from multiple subjects in a non-invasive and continuous manner (beat-to-beat variation = 4.15% – 11.38%). Simultaneously measured carotid local PWV, PTT_R, and PAT_C were compared as markers of BP, and arterial pressure levels were predicted using inter-

subject models. Local PWV was slightly better than PTT_R and PAT_C in terms of tracking SBP (r = 0.74), DBP (r = 0.77) and MAP (r = 0.78). Intra-subject BP–local PWV models derived from post-exercise recovery curve of individual subjects (r > 0.916±0.042) were more accurate in tracking acute changes in BP parameters (RMSE ≤ 2.61 mmHg). Despite the practical feasibility of inter-subject models with population-specific calibration, carotid local PWV offered acceptable accuracy for cuffless BP measurement via intra-subject models with subject-specific calibration. With successful future efforts, the proposed single-source PPG based cuffless BP device could be potentially used for ambulatory and home BP monitoring, hypertension screening, and control.

References

Bogert LWJ and van Lieshout J J 2005 Non-invasive pulsatile arterial pressure and stroke volume changes from the human finger: noninvasive pressure and flow *Experimental Physiology* **90** 437–46

Boutouyrie P, Briet M, Collin C, Vermeersch S and Pannier B 2009 Assessment of pulse wave velocity *Artery Research* **3** 3–8

Bramwell J C and Hill A V 1922 The velocity of the pulse wave in man *Proc. Royal Society of London B* **93** 298–306

Buxi D, Redouté J -M and Yuce M R 2015 A survey on signals and systems in ambulatory blood pressure monitoring using pulse transit time *Physiological Measurement* **36** R1–26

Cai Z G, Zhang J, Zhang J G, Zhao F Y, Yu G Y, Li Y and Ding H S 2008 Evaluation of near infrared spectroscopy in monitoring postoperative regional tissue oxygen saturation for fibular flaps *J. Plast. Reconstr. Aesthetic Surg.* **61** 289–96

Chiu Y C, Arand P W, Shroff S G, Feldman T and Carroll J D 1991 Determination of pulse wave velocities with computerised algorithms *Am. Heart J.* **121** 1460–70

Delpy D T and Cope M 1997 Quantification in tissue near–infrared spectroscopy *Philosophical Trans. Royal Society of London B* **352** 649–59

Ding X, Zhang Y and Tsang H K 2016 Impact of heart disease and calibration interval on accuracy of pulse transit time–based blood pressure estimation *Physiological Measurement* **37** 227–37

Ding X -R, Zhao N, Yang G -Z, Pettigrew R I, Lo B, Miao F, Li Y, Liu J and Zhang Y -T 2016 Continuous blood pressure measurement from invasive to unobtrusive: celebration of 200th birth anniversary of Carl Ludwig *IEEE J. Biomed. Health Informatics* **20** 1455–65

Faita F, Bruno R M, Gemignani V, Bianchini E and Ghiadoni L 2010 Local carotid pulse wave velocity assessment: a vibrational approach *Artery Research* **4** 171

Fedotov A A 2014 Baseline Drift Filtering for an Arterial Pulse Signal *Measurement Techniques* **57** 91–6

Hermeling E, Reesink K D, Reneman R S and Hoeks A P 2007 Measurement of local pulse wave velocity: effects of signal processing on precision *Ultrasound Med. Biol.* **33** 774–81

Hermeling E, Reesink K D, Hoeks A P G and Reneman R S 2010 Potentials and pitfalls of local PWV measurements *American J. Hypertension* **23** 934

Kamal A A R, Harness J B, Irving G and Mearns A J 1989 Skin photoplethysmography – a review *Comput. Methods. Programs. Biomed.* **28** 257–69

Kazanavicius E, Gircys R, Vrubliauskas A and Lugin S 2005 Mathematical methods for determining the foot point of the arterial pulse wave and evaluation of proposed methods *Information Technology and Control* **34** 29–36

Lindberg L G, Sveider P and Oberg P A 1992 Optical properties of blood in motion *Proc. SPIE Optical Fibers in Medicine VII* **1649** 1649–55

Martin S L -O, Carek A M, Kim C -S, Ashouri H, Inan O T, Hahn J -O and Mukkamala R 2016 Weighing scale-based pulse transit time is a superior marker of blood pressure than conventional pulse arrival time *Scientific Reports* **6** 1–8

McCarthy B M, Vaughan C J, O'Flynn B, Mathewson A and Ó Mathúna C 2013 An examination of calibration intervals required for accurately tracking blood pressure using pulse transit time algorithms *J. Human Hypertension* **27** 744–50

Mukkamala R, Hahn J -O, Inan O T, Mestha L K, Kim C -S, Toreyin H and Kyal S 2015 Toward ubiquitous blood pressure monitoring via pulse transit time: theory and practice *IEEE Trans. Biomed. Eng.* **62** 1879–1901

Nabeel P M, Joseph J and Sivaprakasam M 2017 A magnetic plethysmograph probe for local pulse wave velocity measurement *IEEE Trans. Biomed. Circuits Syst.* **11** 1065–76

Pereira T, Correia C and Cardoso J 2015 Novel methods for pulse wave velocity measurement *J. Medical and Biological Engineering* **35** 555–65

Peter L, Noury N and Cerny M 2014 A review of methods for non-invasive and continuous blood pressure monitoring: pulse transit time method is promising? *IRBM* **35** 271–82

Poon C C, Zhang Y -T, Wong G and Poon W S 2008 The beat-to-beat relationship between pulse transit time and systolic blood pressure IEEE *Int. Conf. Information Technology and Applications in Biomedicine (Shenzhen)* pp 342–3

Reusz G S, Cseprekal O, Temmar M, Kis É, Cherif A B, Thaleb A, Fekete A, Szabó A J, Benetos A and Salvi P 2010 Reference values of pulse wave velocity in healthy children and teenagers *Hypertension* **56** 217–24

Salvi P, Magnani E, Valbusa F, Agnoletti D, Alecu C, Joly L and Benetos A 2008 Comparative study of methodologies for pulse wave velocity estimation *J. Hum. Hypertens.* **22** 669–77

Solà J, Vetter R, Renevey P, Chételat O, Sartori C and Rimoldi S F 2009 Parametric estimation of pulse arrival time: a robust approach to pulse wave velocity *Physiological Measurement* **30** 603–15

Sorensen G L, Jensen J B, Udesen J, Holfort I K and Jensen J A 2008 Pulse wave velocity in the carotid artery *IEEE Ultrasonics Symposium (Beijing)* pp 1386–9

Westenberg J J, van Poelgeest E P, Steendijk P, Grotenhuis H B, Jukema J W and de Roos A 2012 Bramwell-Hill modeling for local aortic pulse wave velocity estimation: a validation study with velocity-encoded cardiovascular magnetic resonance and invasive pressure assessment *J. Cardiovascular Magnetic Resonance* **14** 2–10